Silicon homo-heterojunction solar cells: A promising candidate to realize high performance more stably

Miao Tan,[1] Sihua Zhong,[1,a] Wenjie Wang,[1] and Wenzhong Shen[1,2,a]
[1]*Institute of Solar Energy, and Key Laboratory of Artificial Structures and Quantum Control (Ministry of Education), School of Physics and Astronomy, Shanghai Jiao Tong University, Shanghai 200240, People's Republic of China*
[2]*Collaborative Innovation Center of Advanced Microstructures, Nanjing 210093, People's Republic of China*

(Received 30 June 2017; accepted 18 August 2017; published online 28 August 2017)

We have investigated the influences of diverse physical parameters on the performances of a silicon homo-heterojunction (H-H) solar cell, which encompasses both homojunction and heterojunction, together with their underlying mechanisms by the aid of AFORS-HET simulation. It is found that the performances of H-H solar cell are less sensitive to (i) the work function of the transparent conductive oxide layer, (ii) the interfacial density of states at the front hydrogenated amorphous silicon/crystalline silicon (a-Si:H/c-Si) interface, (iii) the peak dangling bond defect densities within the p-type a-Si:H (p-a-Si:H) layer, and (iv) the doping concentration of the p-a-Si:H layer, when compared to that of the conventional heterojunction with intrinsic thin layer (HIT) counterparts. These advantages are due to the fact that the interfacial recombination and the recombination within the a-Si:H region are less affected by all the above parameters, which fundamentally benefit from the field-effect passivation of the homojunction. Therefore, the design of H-H structure can provide an opportunity to produce high-efficiency solar cells more stably.
[http://dx.doi.org/10.1063/1.4993677]

I. INTRODUCTION

Amorphous silicon/crystalline silicon (a-Si/c-Si) heterojunction solar cells have attracted considerable attention in the recent decade, mainly due to their small temperature coefficient, simple fabrication process and high open-circuit voltage (V_{OC}) benefitted from the large difference in Fermi energy of the two materials.[1–5] In order to passivate the c-Si surface, a thin intrinsic hydrogenated amorphous silicon (i-a-Si:H) layer is generally inserted between the doped a-Si layer and the c-Si substrate, forming the heterojunction with intrinsic thin layer (HIT) solar cells. According to the latest report, Kaneka Corp. has realized an efficiency as high as 25.1% on the HIT solar cell[5] and then achieved a record efficiency of 26.6% on a large-area (180 cm^2) HIT solar cell by being incorporated with interdigitated back contact technique.[6] Although the HIT solar cells have been demonstrated to be highly efficient, in mass production, it is hard to fabricate the HIT solar cells with excellent performances stably because their performances are strongly affected by various parameters. Lots of investigations have indicated that inappropriate work function of the transparent conductive oxide (TCO) layer will lead to a dramatical degradation of the performances of HIT solar cells, because the band bending in the emitter strongly depends on the work function of the TCO layer and the emitter.[7–11] The HIT solar cell performances are also quite sensitive to the interfacial density of states (DOS).[12–16] Hernandez *et al.*,[16] demonstrated that the cell performances decline significantly when the interfacial DOS exceeds 1×10^{11} cm^{-2}, while the cell efficiency can be improved to nearly 23%

[a]Corresponding author, E-mail: zhongsh@sjtu.edu.cn, wzshen@sjtu.edu.cn

if the interfacial DOS is controlled below 5×10^{10} cm^{-2}. Additionally, other parameters, such as the doping concentration of the hydrogenated amorphous silicon (a-Si:H) layer and defect states within it, greatly influence the solar cell performances since they directly determine the Fermi energy position in the a-Si:H layer and thus affect the built-in potential of the solar cell.[1,17–20] Therefore, improving the stability of the performances of the heterojunction solar cell while keeping its high efficiency become urgent and are of high significance for mass production.

We have previously presented that the silicon homo-heterojunction (H-H) solar cell, which simultaneously contains homojunction and heterojunction, exhibits better tolerance for the interfacial DOS as compared to the HIT solar cell by AFORS-HET simulation.[21] In addition, it was found that the H-H solar cell shows a much higher fill factor (*FF*). With these two advantages, even if considering the fact that the interfacial DOS of the H-H solar cell is much higher, for example two magnitudes higher, the H-H solar cell can still realize the efficiency as high as that of the HIT solar cell but has a better stability. It should be noted that Hekmatshoar *et al.*,[22] have already experimentally demonstrated that the H-H solar cell on a p-type c-Si (p-c-Si) substrate is less sensitive to the interfacial DOS and has a higher *FF*. Besides, it has been reported that the advantages of the H-H structure will still be retained if an i-a-Si:H layer is inserted to reduce the interfacial DOS.[23,24] Nevertheless, up to now, all the previous studies on the H-H solar cell are mainly focused on the sensitivity of the interfacial DOS and it is still unknown how other fabricating parameters affect the cell performances.

In this study, we have investigated the impacts of (i) the work function of TCO layer (WF_{TCO}), (ii) the total interfacial DOS (D_{it}) at the front a-Si:H/c-Si interface (hetero-interface), (iii) the peak dangling bond defect densities (N_{tr}) within the p-type a-Si:H (p-a-Si:H) layer, and (iv) the doping concentration (N_a) of the p-a-Si:H layer on the performances of the H-H solar cell with a structure of p-a-Si:H/p-c-Si/n-type c-Si (n-c-Si) substrate/i-a-Si:H/n-type a-Si:H (n-a-Si:H) by the aid of AFORS-HET software. We have excitingly found that, as compared with the HIT counterparts, the H-H solar cell is much insensitive to all the above parameters. As a result, the H-H solar cell has better performances in the whole range of each above parameter. Furthermore, we identify that the physical origins behind the advantages of the H-H solar cell are the decreased interfacial recombination and the reduced recombination within the a-Si:H region, which are fundamentally ascribed to the field-effect passivation from the homojunction.

II. STRUCTURES OF SOLAR CELLS AND SIMULATION DETAILS

Numerical simulations were carried out by utilizing the simulation software AFORS-HET, which is based on solving the one-dimensional Poisson equation and the continuity equations[7] and has been proven to be an effective and convenient way to analyze the influences of various parameters on the performances of heterojunction solar cells.[12] The simulated HIT cell structure, as depicted in Fig. 1(a), is TCO/p-a-Si:H/i-a-Si:H/n-c-Si substrate/i-a-Si:H/n-a-Si:H/TCO. Fig. 1(b) shows the structure of the H-H solar cell, namely: TCO/p-a-Si:H/p-c-Si/n-c-Si substrate/i-a-Si:H/n-a-Si:H/TCO. A thin i-a-Si:H layer is further inserted between the p-a-Si:H layer and p-c-Si layer, labeled as H-I-H solar cell and presented in Fig. 1(c).

In the simulations, parasitic absorption in the 80 nm thick TCO layer was ignored. The back contact was assumed to be flat band in order to neglect the influence of band bending at the rear contact, while the band bending at the front contact formed between TCO and p-a-Si:H layer was carefully taken into account by changing the WF_{TCO}. Fig. 1(d)–(f) shows gap state distributions of p-a-Si:H layer, i-a-Si:H buffer layer and n-a-Si:H BSF layer. The density of localized states in a-Si:H layers is mainly composed of exponential band tail defect states and Gaussian distributed dangling bond states. Recombination centers were modeled with 5×10^{11} cm^{-3} and 1×10^{9} cm^{-3} neutral defects at 0.56 eV above the valence band in the p-c-Si layer and n-c-Si layer,[23] respectively. At the front hetero-interface, defects were introduced using a Gaussian distributed DOS with the maximum at the midgap of c-Si.[17,21,25] Electrons and holes capture cross sections were equal to 1×10^{-15} cm^2.[21] In order to focus on the front side of the solar cells, the back hetero-interface was neglected during the simulations.

Regarding the carriers transport across the hetero-interface, thermionic emission model with tunneling model is adopted.[23] The surface recombination velocities of electrons and holes on both

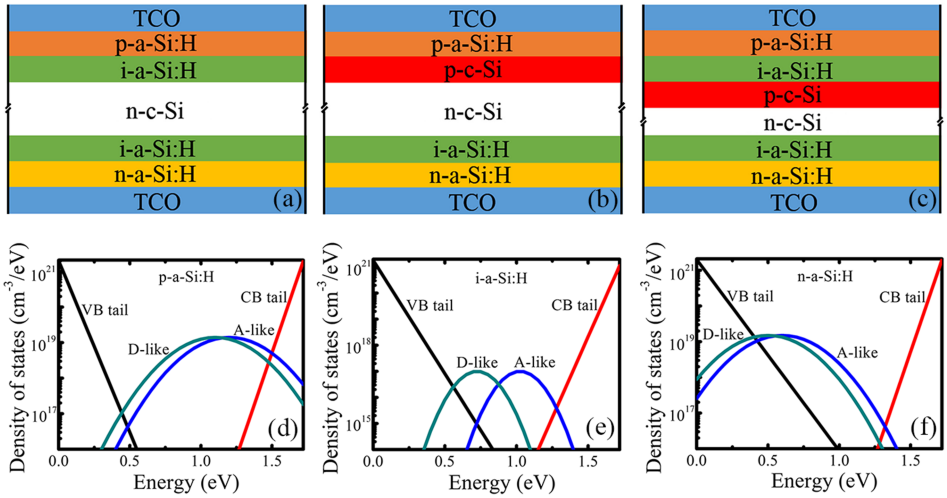

FIG. 1. Schematic diagrams of (a) the HIT, (b) the H-H and (c) the H-I-H solar cells. (d)-(f) The gap state distributions of different types of a-Si:H layers in the simulations. A-like and D-like represent acceptor-like and donor-like dangling bonds, respectively. VB and CB denote valence band and conduction band, respectively.

sides were set to 1×10^{7} cm·s^{-1}. More details of the parameters used in the simulations are listed in Table I, which were mainly referred to the previous works.[7,21,26] We varied the value of the (i) WF_{TCO}, (ii) D_{it} at the front hetero-interface, (iii) N_{tr} within the p-a-Si:H layer and (iv) N_a of the p-a-Si:H layer to investigate how they affect the performances of the simulated solar cells. Only one parameter was varied at one time while other parameters kept at the initial values. The initial values of the above parameters were set to 5.3 eV, 1×10^{12} cm^{-2}, 1.4×10^{19} cm^{-3}/eV, 7.5×10^{18} cm^{-3}, respectively. Simulation results presented in this study were obtained under AM1.5 solar spectrum with a power density of 100 mW/cm^2 and at 25 °C.

III. SIMULATION RESULTS AND DISCUSSION

A. Influences of WF_{TCO} and D_{it} on the performances of simulated solar cells

As the first step of our study, we have analyzed the influences of both the WF_{TCO} and D_{it} on the V_{OC} as well as the conversion efficiency (η) of the H-H and HIT solar cells. During the simulations, WF_{TCO} varies in the range of 5.1-5.5 eV while D_{it} varies from 1×10^{10} cm^{-2} to 5×10^{12} cm^{-2}. As depicted in Fig. 2(a)–(c), V_{OC} decreases with increasing D_{it} when WF_{TCO} keeps constant and obvious improvement in V_{OC} is observed with increasing WF_{TCO} when D_{it} keeps constant. From Fig. 2(d)–(f), it is also noted that the dependence of η on WF_{TCO} and D_{it} follows the same trends as V_{OC}. The decrease in V_{OC} with increasing D_{it} can be explained by the enhanced recombination possibility, since the interface defect states work as recombination centers for photo-generated carriers. WF_{TCO} has also been considered as a crucial factor in a-Si/c-Si heterojunction solar cells due to the fact that WF_{TCO} determines the electrical TCO/p-a-Si:H Schottky contact properties and the band bending in the a-Si:H/c-Si junction region.[8,27,28] As shown in Fig. 2(g) and (h), higher WF_{TCO} leads to stronger band bending at both the TCO/a-Si:H contact and the hetero-interface, which is beneficial for photo-generated holes to be collected by the front electrode and forming an effective potential barrier for electrons at the front hetero-interface. As a result, the carrier recombination at the hetero-interface is greatly reduced and hence the V_{OC} increases.

When observing Fig. 2 more carefully, it can be found that both the V_{OC} and η of the H-H solar cell present better tolerance for D_{it} than those of the HIT solar cell, which is consistent with our previous study.[21] In addition, the V_{OC} and η of the H-H solar cell are also less sensitive to WF_{TCO}. Therefore, with the advantage of better tolerance for both the WF_{TCO} and D_{it}, it is not such necessary to adopt fairly rigorous process to optimize the WF_{TCO} and D_{it} in production lines, which is beneficial to produce heterojunction solar cells with more stable performances. Here, we want to clarify that for

TABLE I. Parameter values adopted in the simulations. CB and VB are conduction band and valence band, respectively; and D-like and A-like represent donor-like and acceptor-like, respectively.

Parameters	p-a-Si:H	i-a-Si:H	n-a-Si:H	n-c-Si	p-c-Si
Layer thickness (cm)	5×10^{-7}	5×10^{-7}	5×10^{-7}	1.8×10^{-2}	1×10^{-6}
Dielectric constant	11.9	11.9	11.9	11.9	11.9
Electron affinity (eV)	3.90	3.90	3.90	4.05	4.05
Mobility band gap (eV)	1.72	1.72	1.72	1.12	1.096
Optical band gap (eV)	1.72	1.72	1.72	1.12	1.096
Doping concentration of acceptors (cm^{-3})	1.0×10^{17}–1.0×10^{19}	0	0	0	1.0×10^{18}
Doping concentration of donors (cm^{-3})	0	0	1.0×10^{19}	1.16×10^{15}	0
Effective conduction band density (cm^{-3})	1.0×10^{20}	1.0×10^{20}	1.0×10^{20}	2.84×10^{19}	1.67×10^{19}
Effective valence band density (cm^{-3})	1.0×10^{20}	1.0×10^{20}	1.0×10^{20}	2.68×10^{19}	1.575×10^{19}
Electron (hole) mobility (cm^2/Vs)	20(5)	20(5)	20(5)	1349(464.4)	328.6(170.3)
Total state density in CB tail (cm^{-3})	7.4×10^{19}	4.0×10^{19}	7.4×10^{19}	—	—
Total state density in VB tail (cm^{-3})	9.0×10^{19}	9.0×10^{19}	1.62×10^{20}	—	—
CB tail(VB tail) Urbach energy (eV)	0.037(0.045)	0.035(0.050)	0.037(0.081)	—	—
Capture cross section for CB tail (cm^2)	7×10^{-16}(e) / 7×10^{-16}(h)	1×10^{-12}(e) / 1×10^{-12}(h)	7×10^{-16}(e) / 7×10^{-16}(h)	—	—
Capture cross section for VB tail (cm^2)	7×10^{-16}(e) / 7×10^{-16}(h)	1×10^{-14}(e) / 1×10^{-14}(h)	7×10^{-16}(e) / 7×10^{-16}(h)	—	—
Maximum D-like Gaussian state density (cm^{-3}/eV)	5.0×10^{18}–2.5×10^{19}	1.0×10^{17}	1.5×10^{19}	—	—
Maximum A-like Gaussian state density (cm^{-3}/eV)	5.0×10^{18}–2.5×10^{19}	1.0×10^{17}	1.5×10^{19}	—	—
Gaussian peak energy for donors (eV)	1.10	0.725	0.50	—	—
Gaussian peak energy for acceptors (eV)	1.20	1.025	0.60	—	—
Standard deviation of Gaussian for donors (eV)	0.21	0.10	0.21	—	—
Standard deviation of Gaussian for acceptors (eV)	0.21	0.10	0.21	—	—
Capture cross section for D-like Gaussian state (cm^2)	3×10^{-14}(e) / 3×10^{-15}(h)	1×10^{-14}(e) / 1×10^{-14}(h)	3×10^{-14}(e) / 3×10^{-15}(h)	—	—
Capture cross section for A-like Gaussian state (cm^2)	3×10^{-15}(e) / 3×10^{-14}(h)	1×10^{-12}(e) / 1×10^{-12}(h)	3×10^{-15}(e) / 3×10^{-14}(h)	—	—

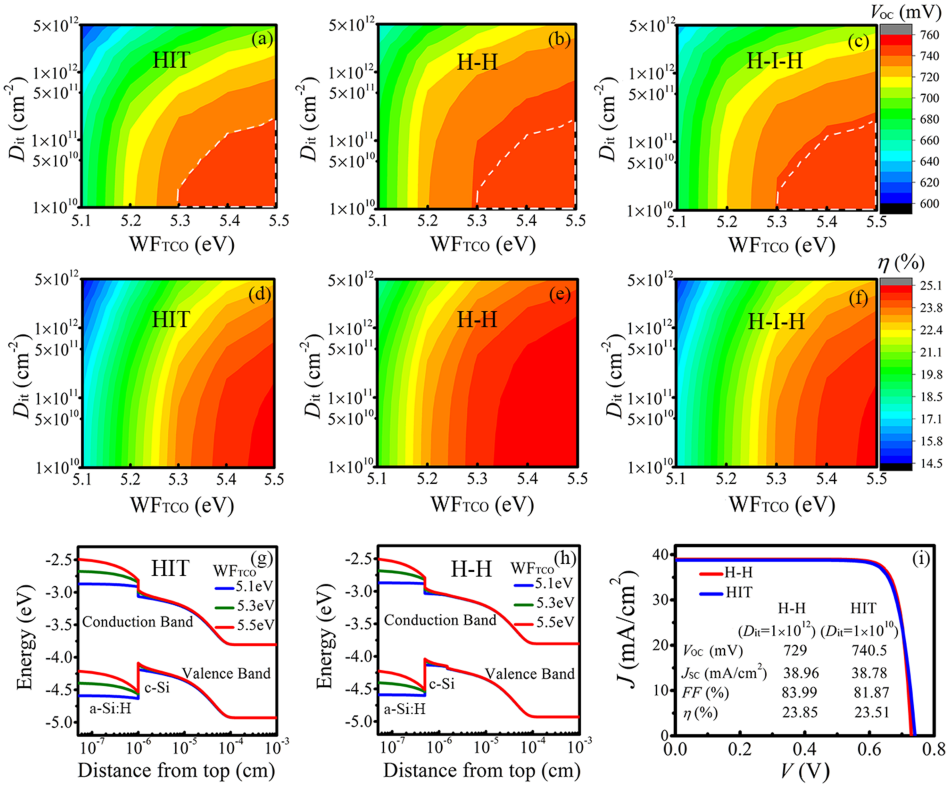

FIG. 2. Dependence of the V_{OC} on WF_{TCO} and D_{it} for the (a) HIT, (b) H-H and (c) H-I-H solar cells. Dependence of the η on WF_{TCO} and D_{it} for the (d) HIT, (e) H-H and (f) H-I-H solar cells. Energy band diagrams at equilibrium of the (g) HIT and (h) H-H solar cells with different WF_{TCO}. (i) Comparison of current density-voltage (J-V) characteristics for the H-H solar cell (D_{it}=1×10^{12} cm^{-2}) and the HIT solar cell (D_{it}=1×10^{10} cm^{-2}) under AM1.5 illumination.

the H-H solar cell, even if considering its higher D_{it} than that of the HIT solar cell, it still has a higher or comparable η. For example, when the D_{it} of the H-H and HIT solar cells are 1×10^{12} cm^{-2} and 1×10^{10} cm^{-2}, respectively (namely, the D_{it} of the H-H solar cell is 100 times larger), the η of the H-H solar cell is still a little higher than that of the HIT solar cell, as shown in Fig. 2(i). This advantage is attributed to the better tolerance of D_{it} and the higher FF caused by the absence of i-a-Si:H layer, which has been explained in detail in our previous study.[21] It should be pointed out that Hekmatshoar *et al.*,[22] have already experimentally demonstrated the better performances of the H-H solar cell than that of the HIT solar cell on a p-c-Si substrate. Moreover, based on the concept of H-H structure, a thin layer of i-a-Si:H film can be further inserted between the p-c-Si layer and p-a-Si:H layer, namely H-I-H, to reduce the D_{it}. As shown in Fig. 2, the performances of the H-I-H solar cell are also less sensitive to both the WF_{TCO} and D_{it} compared to those of the HIT solar cell, but the superiority is not as conspicuous as the H-H solar cell. Therefore, to fully display the benefit of the H-H concept, we will only focus on the comparison of the H-H solar cell and HIT solar cell in the following study.

It is interesting to observe that the H-H and HIT solar cells have a comparable V_{OC} when the values of WF_{TCO} and D_{it} are within the region surrounded by white dashed lines, as shown in Fig. 2(a) and (b), whereas the H-H solar cell exhibits a higher V_{OC} when the values of WF_{TCO} and D_{it} are outside the region. In order to develop an in-depth understanding of this phenomenon, comparisons of electric field and carrier concentration between the H-H and HIT solar cells are shown in Fig. 3(a) and (b) at an external voltage of 0.6 V. Here, the values of WF_{TCO} and D_{it} are set as 5.2 eV and 1×10^{12} cm^{-2}, respectively, and it should be noted that the results discussed below will not change even if the external voltage is set at other values. It is evident that the electric field of the H-H solar cell on the c-Si substrate side and at the hetero-interface is higher than that of the HIT solar cell. Hence it is beneficial for holes but detrimental for electrons to reach the hetero-interface, resulting in a higher

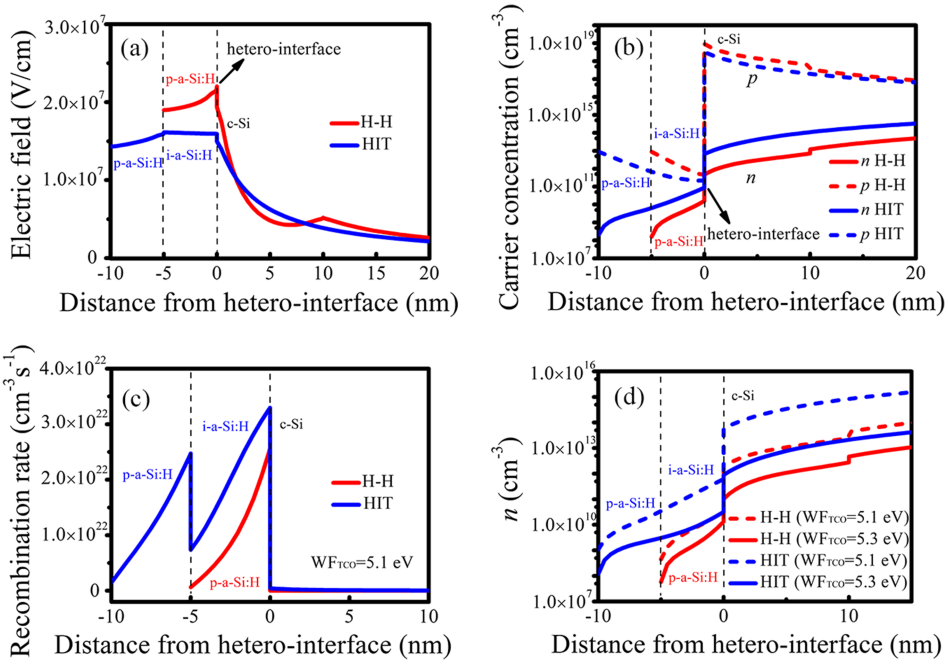

FIG. 3. Comparisons of (a) electric field and (b) carrier concentration between the H-H and HIT solar cells with the WF_{TCO}=5.2 eV and the D_{it}=1×10^{12} cm^{-2}. (c) Comparison of recombination rate between the H-H and HIT solar cells without D_{it} under the WF_{TCO}=5.1 eV. (d) Comparison of n between the H-H and HIT solar cells without D_{it} under different WF_{TCO}. These parameters are obtained under an external voltage of 0.6 V.

hole density (p) and a lower electron density (n) at the hetero-interface, as presented in Fig. 3(b). Since carrier recombination simultaneously involves both types of carriers, the larger difference in the n and p will lead to a lower interfacial recombination. This is known as the field-effect passivation. The field-effect passivation on the interface well explains why the H-H solar cell is less sensitive to D_{it}.[21] Besides, it also adequately explains the better tolerance of WF_{TCO} at a high D_{it}, which is the condition that interfacial recombination dominates the V_{OC}. When the WF_{TCO} decreases, the band bending of the depletion region reduces and the barrier potential for electrons becomes lower. So the n at the hetero-interface of the HIT solar cell is greatly increased, while that of the H-H solar cell is less influenced and keeps a lower value due to the field-effect passivation from the homojunction. As a result, the V_{OC} of the H-H solar cell is higher and shows a better tolerance for the WF_{TCO}. Interestingly, even if D_{it} becomes as low as 1×10^{10} cm^{-2}, the H-H solar cell also performs a superior V_{OC} when the WF_{TCO} is lower than 5.3 eV. Note that, in such a case with a low D_{it}, the recombination at the interface is not the crucial factor to determine the V_{OC} of a solar cell and thus the higher V_{OC} of the H-H solar cell cannot be attributed to the lower n at the hetero-interface as in the high D_{it} condition. This indicates that the lower interfacial recombination is not the only reason for the H-H solar cell to realize the higher V_{OC} with respect to the HIT solar cell.

In order to figure out other reasons, we have modeled the dependence of V_{OC} on the WF_{TCO} for the two types of solar cells without D_{it} (namely D_{it}=0) to totally exclude the influence of the interfacial recombination, as listed in Table II. When WF_{TCO}<5.3 eV, the H-H solar cell exhibits a superior V_{OC} than the HIT counterparts. Moreover, the V_{OC} of the H-H solar cell is less sensitive to WF_{TCO} when WF_{TCO} varies in the range of 5.1-5.3 eV. Through integrating the recombination rate as a function of position, we can obtain the total recombination within the a-Si:H region ($R_{a\text{-}Si:H}$) of the both types of solar cells (listed in Table II). When the WF_{TCO} is 5.1 eV, the electrons in the a-Si:H region are much less for the H-H solar cell, as shown in Fig. 3(d), because the electric field within the homojunction can strongly drag electrons back into the c-Si substrate. As a consequence, the $R_{a\text{-}Si:H}$ of the H-H solar cell (4.97×10^{15} cm^{-2}s^{-1}) is nearly an order of magnitude lower than that of the HIT solar cell (1.60×10^{16} cm^{-2}s^{-1}) and thus the H-H solar cell possesses a higher V_{OC} in comparison with the HIT solar cell. Besides, for the H-H solar cell, the less variation of the n in the a-Si:H region

TABLE II. Effects of WF_{TCO} on the V_{OC} and $R_{a\text{-}Si:H}$ of the H-H and HIT solar cells (D_{it}=0).

	V_{OC} (mV)		$R_{a\text{-}Si:H}$ ($cm^{-2}s^{-1}$)	
WF_{TCO} (eV)	H-H	HIT	H-H	HIT
5.1	682	664	4.97×10^{15}	1.60×10^{16}
5.2	730	719	3.18×10^{15}	4.16×10^{15}
5.3	741	741	2.31×10^{15}	2.75×10^{15}
5.4	743	743	1.82×10^{15}	2.17×10^{15}
5.5	744	744	1.51×10^{15}	1.86×10^{15}

(see Fig. 3(d)) incurs the less variation of the $R_{a\text{-}Si:H}$ with WF_{TCO} in the range of 5.1-5.3 eV, which well explains the less sensitivity of V_{OC} to WF_{TCO}.

By the above analysis, we can draw a conclusion that the better tolerance of WF_{TCO} for the H-H solar cell can be explained by (i) the less variation of the interfacial recombination at a high D_{it} and (ii) the less variation of the $R_{a\text{-}Si:H}$ when the D_{it} is considerably low. Both of them fundamentally benefit from the field-effect passivation within the homojunction.

B. Influences of N_{tr} on the performances of simulated solar cells

Subsequently, the influences of N_{tr} within the p-a-Si:H layer on the performances of the H-H solar cell and the HIT solar cell have been investigated, which is illustrated in Fig. 4. Here, N_{tr} varies from 5×10^{18} cm^{-3}/eV to 2.5×10^{19} cm^{-3}/eV, which is reasonable according to the experimental report.[29] As can be seen from Fig. 4(a), although a higher N_{tr} leads to a lower V_{OC} for both the H-H solar cell and HIT solar cell due to the enhanced carrier recombination within the p-a-Si:H layer, the V_{OC} of the H-H solar cell is much less sensitive to the N_{tr} at either a high D_{it} ($D_{it}=1\times10^{12}$ cm^{-2}) or a low D_{it} ($D_{it}=1\times10^{10}$ cm^{-2}). Hence the V_{OC} of the H-H solar cell keeps a higher value in the whole range of N_{tr}. Similar to the V_{OC}, Fig. 4(b) shows that the FF of the H-H solar cell also keeps a higher value in the whole range of N_{tr} and is less sensitive to N_{tr} when compared to that of the HIT solar

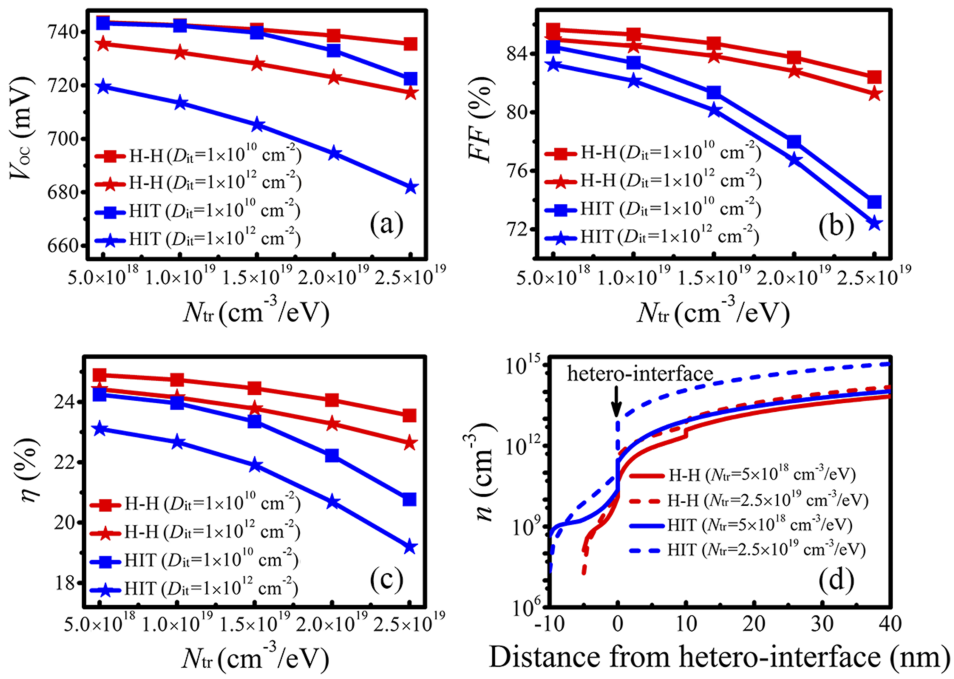

FIG. 4. Effects of N_{tr} in the p-a-Si:H layer on (a) V_{OC}, (b) FF and (c) η of the H-H and HIT solar cells under two different D_{it}. (d) Comparison of n between the H-H and HIT solar cells under two different values of N_{tr}.

cell. As a result, the η of the H-H solar cell is also less sensitive to N_{tr}, as shown in Fig. 4(c). Hence, the η of the H-H solar cell with D_{it}=1×10^{12} cm^{-2} and N_{tr}=2.5×10^{19} cm^{-3}/eV is 1.87% absolutely higher than that of the HIT solar cell with D_{it}=1×10^{10} cm^{-2} and N_{tr}=2.5×10^{19} cm^{-3}/eV.

It is believed that the N_{tr} in the doped a-Si:H layer is easily affected by dopant gas flow rate and/or hydrogen dilution during deposition[29] and the defects in the doped a-Si:H emitter play an important role in the performances of heterojunction devices.[17,26,30] Therefore, accurate control of the dopant gas flow rate and/or hydrogen dilution is required if the performances of the solar cell are sensitive to the N_{tr}. With the advantage of a better tolerance for N_{tr}, the H-H solar cell provides a new opportunity for photovoltaics to fabricate solar cells with stable and excellent performances.

In order to get an insight into the better tolerance of N_{tr} for the H-H solar cell, electron densities (ns) under two different values of N_{tr} have been extracted from the numerical simulation software. When N_{tr} increases from 5×10^{18} cm^{-3}/eV to 2.5×10^{19} cm^{-3}/eV, the active doping concentration of p-a-Si:H layer decreases[17,31] and the Fermi level in p-a-Si:H layer shifts away from the valence band edge. As a result, the built-in potential reduces and more electrons have the ability to reach the hetero-interface as well as the a-Si:H region. Consequently, the n at the hetero-interface and within the a-Si:H region of the HIT solar cell is greatly increased. However, the electric field of the homojunction can partly compensate the reduced electric field caused by the increased N_{tr} so that the n of the H-H solar cell is less influenced by the N_{tr}. Hence there is a smaller difference in n within the a-Si:H region and at the hetero-interface for the H-H solar cell (as presented in Fig. 4(d)), which leads to a smaller difference in carrier recombination, and thus the V_{OC} as well as the FF.[10]

C. Influences of N_a on the performances of simulated solar cells

Fig. 5(a)–(d) illustrates the effects of the N_a of the p-a-Si:H layer on the performances of the H-H and HIT solar cells. It should be noted that, an increase in N_{tr} with increasing N_a[32,33] is not considered here for simplicity because the influences of N_{tr} on the performances of the H-H and HIT solar cells have been discussed above. Both the V_{OC} and FF are reduced with decreasing N_a due to the weaker built-in electric field in the depletion region,[18,34–36] while higher short-circuit current density (J_{SC}) is observed at a lower N_a owing to the diminished parasitic absorption in the p-a-Si:H layer. As an overall result, the η is found to be reduced when N_a decreases. In Fig. 5(a)–(d), another remarkable characteristic is that all parameters of the H-H solar cell are much insensitive to the N_a and keep higher values in the whole range of N_a. It needs to be pointed out that the doping of boron is rather hard to be accurately controlled during the deposition of p-a-Si:H layer, which results in the unstable N_a and greatly affects the performances of a-Si/c-Si heterojunction solar cells.[19] With respect to this, the better tolerance of N_a for the H-H solar cell is of crucial importance to produce high-performance solar cells stably.

In order to give a clear interpretation on how N_a differently impacts the performances of the H-H and HIT solar cells, their energy band diagrams under different N_a are compared, shown in Fig. 5(e). When the N_a of the p-a-Si:H layer decreases from 1×10^{19} cm^{-3} to 1×10^{18} cm^{-3}, the band bending within the a-Si:H/c-Si junction of the HIT solar cell is greatly reduced, leading to the decreased potential barrier for electrons. Consequently, the n at the hetero-interface of the HIT solar cell is largely increased, as confirmed in Fig. 5(f). In contrast, with the benefit of the homojunction, the band bending within the a-Si:H/c-Si junction of the H-H solar cell is less affected by N_a and hence the n of the H-H solar cell is less influenced by N_a. As a result, the performances of the H-H solar cell are less sensitive to the N_a.

Overall, compared to the HIT counterparts, the reasons why the H-H solar cell shows better tolerance for all the above physical parameters are ascribed to the field-effect passivation from the homojunction, which leads to the less variation of the n, and thus the less affected interfacial recombination and the $R_{a\text{-}Si:H}$. Based on the above results and discussion, it is expected that the concept of H-H structure will also greatly benefit carrier-selective contact solar cells.[37–39] For example, the H-H structure can not only provide an excellent field-effect passivation for the hetero-interface but also help to reduce the sensitivity of cell performances to the work function of the carrier-selective contact materials. Hence a higher and more stable efficiency can be realized for the carrier-selective contact solar cells.

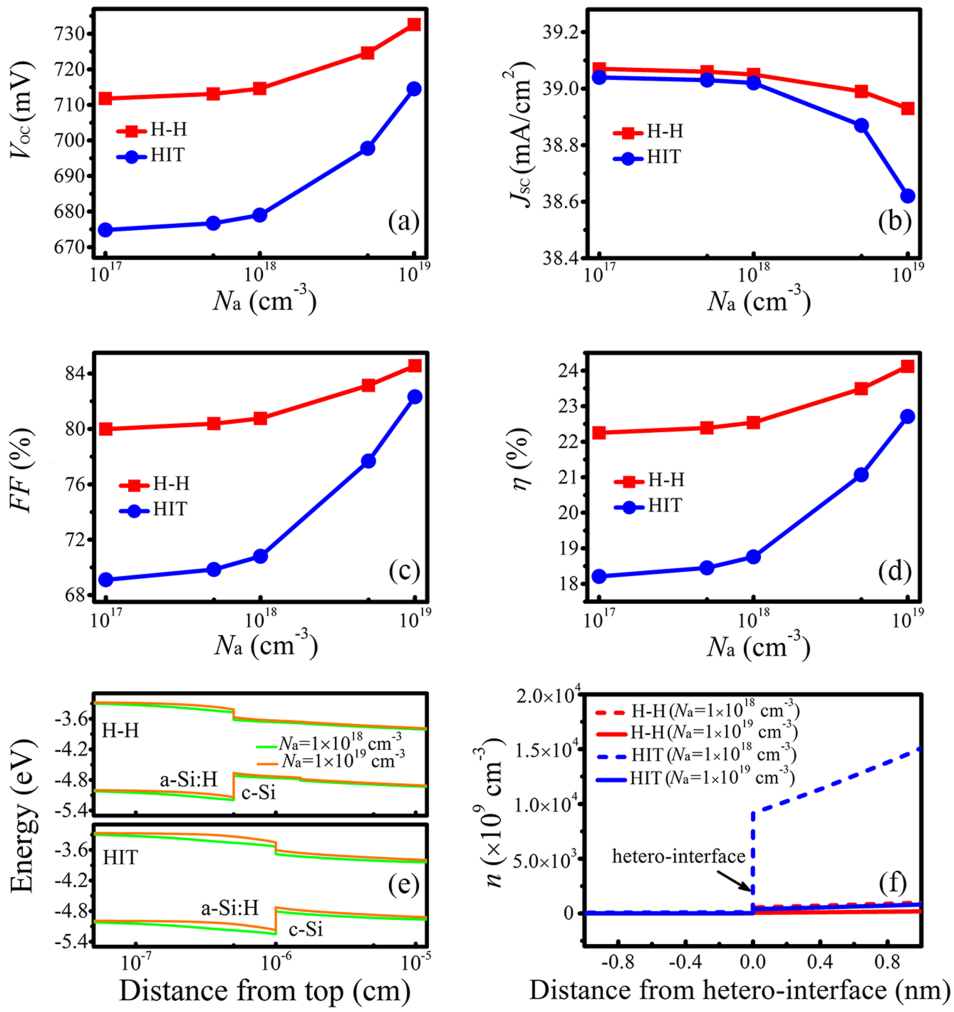

FIG. 5. Variation of (a) V_{OC}, (b) J_{SC}, (c) FF and (d) η as a function of N_a for the H-H and HIT solar cells. (e) Energy band diagrams of the H-H and HIT solar cells with different N_a at 0.6 V. (f) Comparison of n between the H-H and HIT solar cells under two different values of N_a.

IV. CONCLUSIONS

The effects of the WF_{TCO}, D_{it}, N_{tr} within the p-a-Si:H layer and the N_a of the p-a-Si:H layer on the performances of the H-H and HIT solar cells were thoroughly compared using AFORS-HET software. An important finding was that both the V_{OC} and η of the H-H solar cell present better tolerance for the D_{it} and WF_{TCO} due to the field-effect passivation from the homojunction. To be specific, the reason why the H-H solar cell is more insensitive to the WF_{TCO} has been identified to the less variation of the interfacial recombination at a high D_{it} and to the less variation of the $R_{a\text{-}Si:H}$ when the D_{it} is considerably low. Both of them are owing to the fact that less electrons can reach the hetero-interface and the a-Si:H region under the strong electric field within the homojunction and thus the n of the H-H solar cell is less influenced by the WF_{TCO}. Moreover, it was excited to find that, as compared to the HIT counterparts, the H-H solar cell is also less sensitive to both the N_{tr} and N_a of the p-a-Si:H layer. The reason is that the n of the H-H solar cell is less influenced by the N_{tr} or N_a since the electric field within the homojunction can partly compensate the reduced electric field caused by the increased N_{tr} or the decreased N_a. Furthermore, the performances of the H-H solar cell keep higher in the whole range of each parameter. With better tolerance for all the above parameters that greatly influence the HIT cell performances, we believe that the H-H solar cell is promising to be adopted in photovoltaic industry to produce high-efficiency solar cells more stably.

ACKNOWLEDGMENTS

This work was supported by the Natural Science Foundation of China (11474201, 61234005 and 11674225), and China Postdoctoral Science Foundation (15Z102060052 and 16Z102060054).

[1] M. Ghannam, G. Shehadah, Y. Abdulraheem, and J. Poortmans, Sol. Energy Mater. Sol. Cells **132**, 320 (2015).
[2] W. G. J. H. M. van Sark, L. Korte, and F. Roca, *Physics and Technology of Amorphous-Crystalline Heterostructure Silicon Solar Cells* (Springer-Verlag, Berlin, 2012).
[3] S. D. Wolf, A. Descoeudres, Z. C. Holman, and C. Ballif, Green **2**, 7 (2012).
[4] C. Ballif, S. D. Wolf, A. Descoeudres, and Z. C. Holman, Semicond. Semimet. **90**, 73 (2014).
[5] D. Adachi, J. L. Hernández, and K. Yamamoto, Appl. Phys. Lett. **107**, 233506 (2015).
[6] K. Yoshikawa, H. Kawasaki, W. Yoshida, T. Irie, K. Konishi, K. Nakano, T. Uto, D. Adachi, M. Kanematsu, H. Uzu, and K. Yamamoto, Nat. Energy **2**, 17032 (2017).
[7] X. X. Wen, X. B. Zeng, W. G. Liao, Q. S. Lei, and S. Yin, Sol. Energy **96**, 168 (2013).
[8] E. Centurioni and D. Iencinella, IEEE Electron Device Lett. **24**, 177 (2003).
[9] M. Ghannam, Y. Abdulraheem, and G. Shehada, Sol. Energy Mater. Sol. Cells **145**, 423 (2016).
[10] W.-K. Oh, S. Q. Hussain, Y.-J. Lee, Y. Lee, S. Ahn, and J. Yi, Mater. Res. Bull. **47**, 3032 (2012).
[11] M. Rahmouni, A. Datta, P. Chatterjee, J. Damon-Lacoste, C. Ballif, and P. R. I. Cabarrocas, J. Appl. Phys. **107**, 054521 (2010).
[12] Q. Liu, X. J. Ye, C. Liu, and M. B. Chen, Optoelectron. Lett. **6**, 108 (2010).
[13] A. Datta, M. Rahmouni, M. Nath, R. Boubekri, P. R. I. Cabarrocas, and P. Chatterjee, Sol. Energy Mater. Sol. Cells **94**, 1457 (2010).
[14] H. Angermann, E. Conrad, L. Korte, J. Rappich, T. F. Schulze, and M. Schmidt, Mater. Sci. Eng. B **159-160**, 219 (2009).
[15] M. Krichen and A. B. Arab, J. Comput. Electron. **15**, 269 (2016).
[16] N. Hernández-Como and A. Morales-Acevedo, Sol. Energy Mater. Sol. Cells **94**, 62 (2010).
[17] X. Hua, Z. P. Li, W. Z. Shen, G. Y. Xiong, X. S. Wang, and L. J. Zhang, IEEE Trans. Electron Devices **59**, 1227 (2012).
[18] J. Liu, S. H. Huang, and L. He, J. Semicond. **36**, 044010 (2015).
[19] E. Conrad, K. v. Maydell, H. Angermann, C. Schubert, and M. Schmidt, "Optimization of interface properties in a-Si:H/c-Si heterojunction solar cells," in *the 4th IEEE World Conference on Photovoltaic Energy Conversion, Waikoloa, HI* (2006), pp. 1263–1266.
[20] D. Rached and H. M. Yssad, Acta Phys. Pol. A **127**, 767 (2015).
[21] S. H. Zhong, X. Hua, and W. Z. Shen, IEEE Trans. Electron Devices **60**, 2104 (2013).
[22] B. Hekmatshoar, D. Shahrjerdi, and D. K. Sadana, "Novel heterojunction solar cells with conversion efficiencies approaching 21% on p-type crystalline silicon substrates," in *International Electron Devices Meeting, Washington, DC, USA* (2011), pp. 36.6.1-36.6.4.
[23] T. Carrere, R. Varache, D. Muñoz, and J. P. Kleider, J. Renewable Sustainable Energy **7**, 011202 (2015).
[24] T. Carrere, R. Varache, J. L. Perchec, C. Denis, D. Muñoz, and J.-P. Kleider, Energy Procedia **77**, 451 (2015).
[25] C. Leendertz, R. Stangl, T. F. Schulze, M. Schmidt, and L. Korte, Phys. Status Solidi C **7**, 1005 (2010).
[26] Z. Shu, U. Das, J. Allen, R. Birkmire, and S. Hegedus, Prog. Photovoltaics Res. Appl. **23**, 78 (2015).
[27] L. Zhao, C. L. Zhou, H. L. Li, H. W. Diao, and W. J. Wang, Sol. Energy Mater. Sol. Cells **92**, 673 (2008).
[28] M. Bivour, S. Schröer, and M. Hermle, Energy Procedia **38**, 658 (2013).
[29] L. Zhang, U. K. Das, Z. Shu, H. Liu, R. W. Birkmire, and S. S. Hegedus, "Experimental and simulated analysis of p a-Si:H defects on silicon heterojunction solar cells: Trade-offs between V_{OC} and FF," in *the 42nd IEEE Photovoltaic Specialist Conference, New Orleans, LA, USA* (2015).
[30] F. Y. Meng, L. L. Shen, J. H. Shi, L. P. Zhang, J. N. Liu, Y. C. Liu, and Z. X. Liu, Appl. Phys. Lett. **107**, 223901 (2015).
[31] D. Pysch, C. Meinhard, N.-P. Harder, M. Hermle, and S. W. Glunz, J. Appl. Phys. **110**, 094516 (2011).
[32] N. Dwivedi, S. Kumar, A. Bisht, K. Patel, and S. Sudhakar, Sol. Energy **88**, 31 (2013).
[33] S. M. de Nicolás, D. Muñoz, A. S. Ozanne, N. Nguyen, and P. J. Ribeyron, Energy Procedia **8**, 226 (2011).
[34] D. Cheyns, J. Poortmans, P. Heremans, C. Deibel, S. Verlaak, B. P. Rand, and J. Genoe, Phys. Rev. B **77**, 165332 (2008).
[35] C. L. Zhong, K. W. Geng, L. E. Luo, and D. W. Yang, J. Cent. South Univ. **23**, 598 (2016).
[36] L. L. Shen, F. Y. Meng, and Z. X. Liu, Sol. Energy **97**, 168 (2013).
[37] J. Bullock, A. Cuevas, T. Allen, and C. Battaglia, Appl. Phys. Lett. **105**, 232109 (2014).
[38] C. Battaglia, S. M. de Nicolás, S. D. Wolf, X. T. Yin, M. Zheng, C. Ballif, and A. Javey, Appl. Phys. Lett. **104**, 113902 (2014).
[39] Y. M. Wan, C. Samundsett, J. Bullock, T. Allen, M. Hettick, D. Yan, P. T. Zheng, X. Y. Zhang, J. Cui, J. McKeon, A. Javey, and A. Cuevas, ACS Appl. Mater. Interfaces **8**, 14671 (2016).